Axial loading tests and load capacity prediction of slender SHS stub columns strengthened with carbon fiber reinforced polymers

Jai-woo Park[1a] and Jung-han Yoo[*2]

[1] *Gayoon Construction. Co. Ltd., 9-91, Hwayang-dong, Gwangjin-gu, Seoul, 143-130, Republic of Korea*
[2] *School of Architecture, Seoul National University of Science & Technology,*
232 Gongreung-ro, Nowon-gu, Seoul, 139-743, Republic of Korea

Abstract. This paper presents the experimental results of axially loaded stub columns of slender steel hollow square section (SHS) strengthened with carbon fiber reinforced polymers (CFRP) sheets. 9 specimens were fabricated and the main parameters were: width-thickness ratio (b/t), the number of CFRP ply, and the CFRP sheet orientation. From the tests, it was observed that two sides would typically buckle outward and the other two sides would buckle inward. A maximum increase of 33% was achieved in axial-load capacity when 3 layers of CFRP were used to wrap HSS columns of $b/t = 100$ transversely. Also, stiffness and ductility index (DI) were compared between un-retrofitted specimens and retrofitted specimens. Finally, it was shown that the application of CFRP to slender sections delays local buckling and subsequently results in significant increases in elastic buckling stress. In the last section, a prediction formula of the ultimate strength developed using the experimental results is presented.

Keywords: FRP; CFRP; Steel hollow section (SHS); slender section; retrofit; elastic buckling; reduction factor

1. Introduction

Ever since the 1980s, fiber reinforced polymer (hereinafter referred to as FRP) sheets have been widely used as strengthening materials for concrete structures, and a number of studies associated with these materials have been conducted as well. However, the studies or cases of application of FRP in steel structures are extremely rare. In general, although for strengthening methods for steel structures only steel plate methods are used, steel plate itself is a heavy material and, as such, it lacks in terms of construction workability and, while increasing the weight of the structure, it is vulnerable to corrosion. In addition, when steel plate retrofit method is applied, bolts or welding is used to connect to the mother material, and this can be fraught with numerous shortcomings, including deformations to the mother material due to damages to the cross-section

---

∗Corresponding author, Assistant Professor, E-mail: happyjh@seoultech.ac.kr
[a] Director of Engineering Division, Ph.D., E-mail: anm21c@hanmail.net

of the mother material or due to the residual stresses from the heat from welding. Recently, escaping the preconceived notions about the existing steel plate retrofitting methods, led by countries overseas, studies associated with FRP sheets for steel structures are being pursued; and there are many actual cases of application in actual construction sites. Since FRP is a light weight material compared to steel plates and strong resistance to corrosion, it offers simple construction workability. Additionally, its tensile strength is about 10 times higher than that of steel plates; therefore, high reinforcement effects can be expected from small amount of reinforcement. Miller *et al*. (2001), Sallam *et al*. (2010) and Fam *et al*. (2009) conducted studies that, by retrofitting the lower part of the flange of an I-type composite beams using carbon fiber reinforced polymer (CFRP) sheet and glass fiber reinforced polymer (GFRP), improved the flexural performance. Shatt and Fam (2006, 2009) carried out axial load tests by reinforcing long and short columns of rectangular steel tubes; in particular, in short columns it was possible to observe confinement effects on local buckling through retrofitting in the transverse direction and it was possible to verify retrofitting effects that enable withstanding increased buckling loads for long columns through reinforcement in the longitudinal direction. Narmashri *et al*. (2010) even verified retrofitting effects through shear strengthening on the shear zone of I-type beams by using CFRP strips. Teng and Hu (2007) conducted axial load tests on cylindrical steel tube columns retrofitted with GFRP. As a result, it was possible to verify strengthening effects through retrofitting in the transverse direction by delaying local buckling in the outward direction via the confining effects of GFRP. Shatt and Fam (2006, 2009) conducted central compression tests by retrofitting with CFRP in the transverse direction for short columns and in the longitudinal direction for long columns that were each made with SHS steel tubes, and in the case of short columns, it was possible to increase the axial strength by delaying buckling through the confinement effects of CFRP. In the case of long columns, the elastic modulus increased due to CFRP and the Euler buckling load increased, and it was possible to observe an increase in the axial strength as a result. However, in existing studies, the focus has been on the width-thickness ratio of steel tubes only for compact cross-section specimens. Harries *et al*. (2009) conducted an experimental test on enhancing stability of structural steel section using FRP strips. By applying FRP materials, the steel compression member could have the improved global and local buckling behavior. El-Tawil *et al*. (2011) studied on the enhancing stability of steel column with FRP strips. CFRP was used to enhance the plastic hinge region of double-channel members on chord members of a special truss moment frames. From the test, the CFRP could inhibit the local buckling of the channel flanges. Finally, it was concluded that improved behavior of the plastic hinge region as compared to unreinforced specimens.

In our study, unlike the existing studies (Shatt and Fam 2006, 2009, Teng and Hu 2007), we attempt to understand the axial compression behavior of rectangular steel tube columns that are comprised of thin-walled angular steel tubes. The current code such as AISC Standards, etc. in accordance with the width-thickness ratio of steel tubes, there are compact cross-section, non-compact cross-section and slender cross-section, and of these, because of thin-wall cross-section having a relatively large width-thickness ratio, local buckling occurs before reaching the yield strength. And, in order to prevent this, width-thickness ratios that are below a certain limit are applied in the AISC provision (AISC 2005). Recently, with the development of high-strength steel, sufficient strengths are expected to be achieved with small amount of steel cross-sectional area wise and, because of this, more active use of thin-wall steel plates can be expected. Nevertheless, although using thin-wall steel offers advantages of reducing the amount of steel used, local buckling occurs before reaching the yield strength due to relatively large

width-thickness ratios, and there is a shortcoming of significant degradation of strength after the onset of buckling. In our study, in order to increase the compressive strength of steel tube columns comprised of thin walls with a large width-thickness ratio, FRP sheets wrap on the outer walls of steel tubes. Among FRP sheets, CFRP with high strength and excellent structural performance was selected in this study. CFRP wraps on SHS (Square Hollow Section) with 3 types of width-thickness ratios of the slender section mentioned in the AISC provision, axial load tests were conducted. From the test results, structural behaviors were observed, and the strengthening effects, initial stiffness, ductility, etc. were examined.

2. Experimental program

2.1 Fabrication of test specimens and test parameters

The AISC provision (AISC 2005), in accordance with the load conditions and the shape of cross-section, separates in terms of compact cross-section, non-compact cross-section and thin-wall cross-section, and slenderness that becomes the standard for these is referred to as the limit width-thickness ratio.

In order to set the test variables for width-thickness ratio, in this study test variables were selected for cross-sections that have width-thickness ratios higher than the limit width-thickness ratio ($b/t = 1.40\sqrt{E/F_y}$) for non-compact cross-sections for rectangular steel tubes that are under uniform compression; in other words, for slender cross-sections. The variables for specimens were

(a) Bent steel plate	(b) Argon welding

(c) Transverse reinforcement	(d) Longitudinal reinforcement

Fig. 1 Specimen fabrication

Table 1 Specimen List

Specimen label	Size (mm)	b/t (Nominal value)	b/t (Actual value)	Number of reinforcement ply	Fiber orientation
SH60-0T	142.6 × 142.6	60	62.7	-	-
SH60-1T	142.6 × 142.6	60	62.7	1	1T
SH60-3T	142.6 × 142.6	60	62.7	3	3T
SH80-0T	188.6 × 188.6	80	83.6	-	-
SH80-1T	188.6 × 188.6	80	83.6	1	1T
SH80-3T	188.6 × 188.6	80	83.6	3	3T
SH100-0T	234.6 × 234.6	100	104.5	-	-
SH100-3T	234.6 × 234.6	100	104.5	3	3T
SH100-1T1L1T	234.6 × 234.6	100	104.5	3	1T 1L 1T

*SH: Square Hollow, 100 (60, 80): b/t, 1T: 1 transverse reinforcement ply, 1L: 1 longitudinal reinforcement ply

the width-thickness ratio, the number of CFRP ply, and the fiber orientation (transverse and longitudinal). To vary the width-thickness ratios, using a steel plate with 2.3 mm thickness, the width of steel tube was varied and the width-thickness ratio was ranged from 60 to 100 in increments of 20, and a total of 3 types of width-thickness ratios were set as test variables and 9 SHS steel tubes were fabricated. The length of specimens was made to be 3 times of the width, and in order to distribute loads evenly end plates were installed on each end. Although the thickness of steel plate was planned to be 2.3 mm, the actual thickness measured using vernier calipers was shown to be 2.2 mm (Fig. 1(a)). Since thin wall steel plates needed to be welded to prepare specimens, as shown in Fig. 1(b), argon weld with relatively a small amount of deformation was performed. To attach CFRP, first, rust on the steel plate surface was eliminated using sandpaper and afterwards a primer was applied on the surface of steel tubes. First, after applying epoxy on steel tube, CFRP was attached to steel tube, and the overlapping length was made to be about 100 mm. In order to examine the reinforcement effects of CFRP according to the number of reinforcement ply, as shown in Fig. 1(c), except for the control specimen, each of the specimens was reinforced with 1-ply and 3-ply in the transverse direction. Lastly, to understand the effects of the reinforcement direction of CFRP, among the specimens with width-thickness ratio of 100, as shown in Fig. 1(d), on 1 specimen a total of 3-ply of CFRP was applied in the transverse direction, longitudinal direction and transverse direction in alternating fashion, and in this way a total of 9 specimens were fabricated, and after reinforcement, per the reinforcement manufacturer's manuals, the specimens were cured for 10-days. The list of specimens is summarized in Table 1.

2.2 Material test

Material test results for steel plates showed that the yield strength (F_y) was 288 MPa, tensile trength (F_u) 371 MPa and the elongation was 33%. CFRP was manufactured by SK Chemical, and the average thickness was 0.184 mm/ply, and tensile strength was 2696 MPa and the fracture strain was 0.015 and modulus of elasticity was 179.7 GPa. The value for typical thickness of a lamina (a single layer of fabric, wetted with resin and cured) was 0.5 mm-1.0 mm.
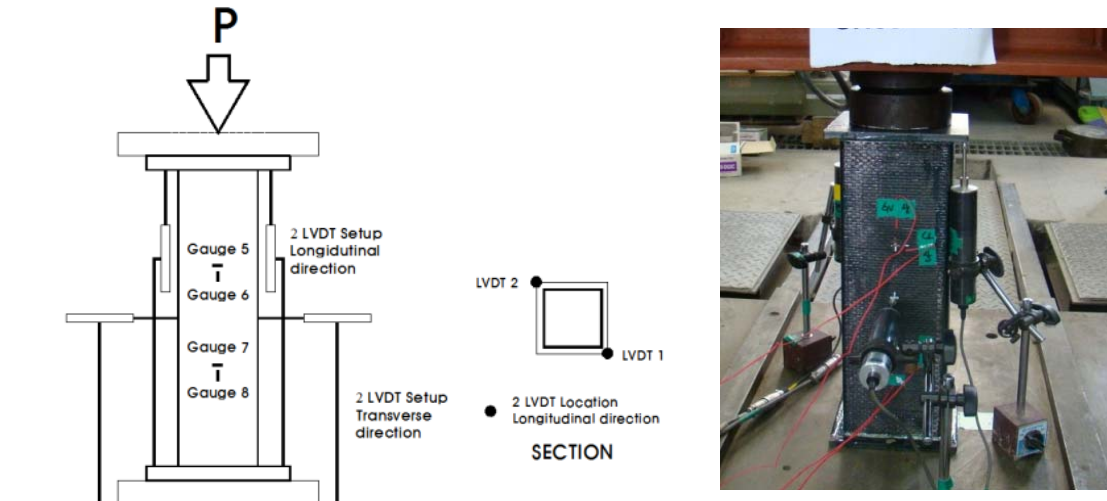
Fig. 2 Test setup

2.3 Test setup and instrumentation

Fig. 2 shows the measurement plan diagram for specimens and specimen setup. To measure displacement in the longitudinal direction, on each corner of the end plates 2 pieces of 50 mm LVDTs were installed and the average of the 2 values was determined to be the longitudinal displacement. To measure displacement in the transverse direction for the central part of a specimen, 2 pieces of 50 mm LVDTs were installed in the transverse direction. In addition, by installing strain gauges at a location between 1/3 spot and 2/3 spot for each of the specimens in the longitudinal direction and transverse direction, strains in the longitudinal direction and the transverse direction were measured, and central compression tests were conducted in a 2000 kN-class UTM.

3. Experimental results

3.1 Specimen failure mode

Fig. 3 shows failure modes under loads for un-retrofitted specimens and retrofitted specimens. Both the reinforced specimens and un-retrofitted specimens, as shown in Figs. 3(a) and (b), symmetrically on 2 sides of the 4 sides an inward local buckling occurred and on the other 2 sides an outward local buckling occurred as they were destroyed. Of these, the specimens retrofitted with CFRP, as shown in Fig. 3(c), on the 2 sides where inward local buckling occurred the steel plate and CFRP was delaminated as they were destroyed. In addition, as shown in Fig. 3(d), although the occurrence of buckling was delayed on the 2 sides where outward local buckling occurred through the confinement effects of CFRP, afterwards, as the range of local buckling increased, CFRP ruptured as it was destroyed.

(a) Control specimen failure

(b) Retrofitted specimen failure
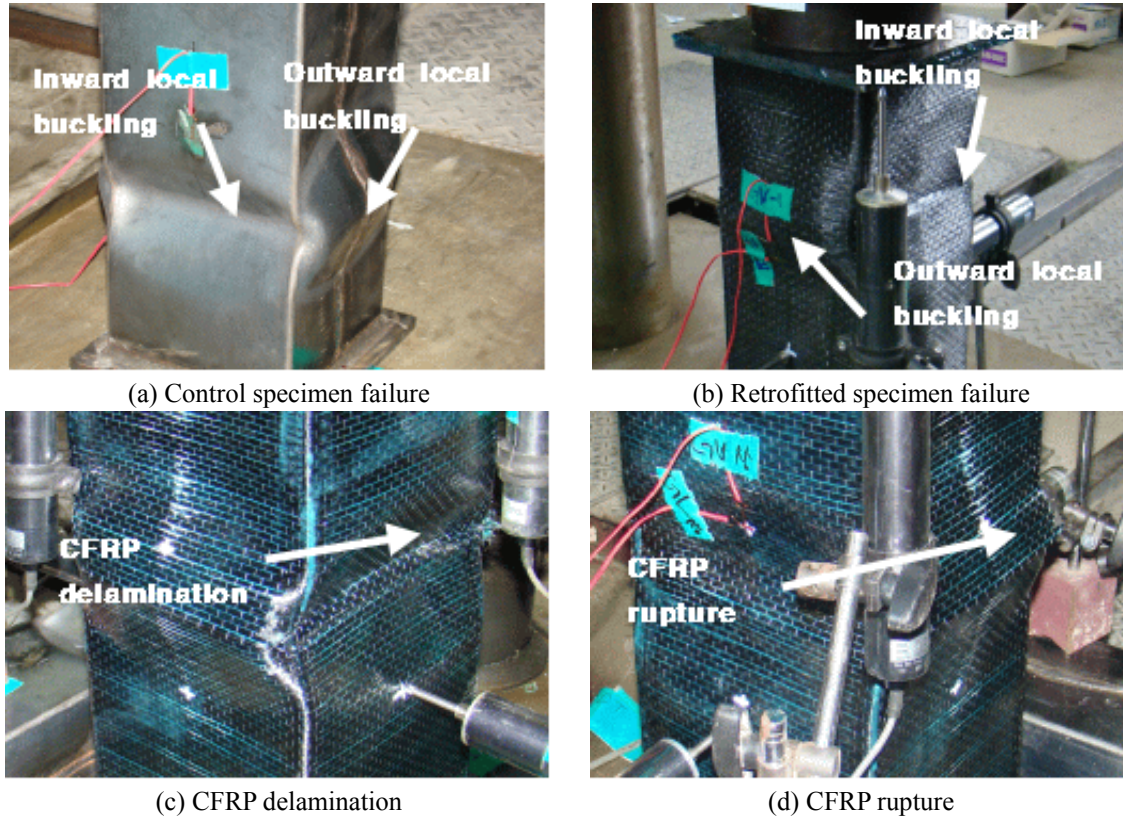
(c) CFRP delamination

(d) CFRP rupture

Fig. 3 Failure mode

3.2 Test results and load-axial displacement curves

In Table 2 the test results and in Fig. 4 the load-axial displacement curves of specimens are summarized. The load-axial displacement curve for each specimen shows the internal strength increasing linearly up to the point of maximum strength and sharply decreasing right after the point of maximum internal strength. The straight line in Fig. 4 represents the yield load (P_y) values, and all the specimens undergo local buckling where the maximum load is reached before the yield load and they show elastic buckling behavior in which the load decreases. In particular, among the specimens with width-thickness ratio of 100, the retrofitted specimens showed a sudden decrease in the load as compared to the other specimens, whereby displaying a brittle behavior. Specimens with large plate width-thickness ratios have relatively small amount of steel plate compared to the cross-section; therefore, they are relatively weaker in terms of local buckling and they become unable to produce ductile behavior after the point of maximum load due to yield of steel plate. However, although the load can be increased through retrofit using CFRP, due to the brittle nature of CFRP, the specimens are subject to the brittleness of CFRP rather than the ductility of steel materials and thereby undergo brittle failure and this can account for the phenomenon of sudden decrease in the load, and this type of phenomenon shows more clearly in specimens with large width-thickness.

Table 2 Summary of test results

| Specimen label		Results	Value of gain or loss	% Gain or loss
SH60-0T	Maximum load (kN)	227.0	Control	Control
	Displacement (mm)	2.081		
	Stiffness (kN/mm)	328.7		
	Ductility	6.969		
SH60-1T	Maximum load (kN)	271.0	44.0	19.4
	Displacement (mm)	0.995	-1.086	
	Stiffness (kN/mm)	304.72	-23.98	-7.3
	Ductility	3.198	-3.771	-54.2
SH60-3T	Maximum load (kN)	290.0	27.8	27.8
	Displacement (mm)	0.740	-1.341	
	Stiffness (kN/mm)	358.3	29.6	9.00
	Ductility	3.072	-3.897	-55.54
SH80-0T	Maximum load (kN)	239.0	Control	Control
	Displacement (mm)	1.838		
	Stiffness (kN/mm)	224.1		
	Ductility	3.387		
SH80-1T	Maximum load (kN)	267.0	28.0	12.0
	Displacement (mm)	1.398	-0.44	
	Stiffness (kN/mm)	222.5	-1.6	10.03
	Ductility	3.111	-0.276	35.41
SH80-3T	Maximum load (kN)	298.0	59.0	25.0
	Displacement (mm)	2.807	0.249	
	Stiffness (kN/mm)	200.5	-23.6	-5.00
	Ductility	3.559	0.172	29.04
SH100-0T	Maximum load (kN)	280.0	Control	Control
	Displacement (mm)	1.273		
	Stiffness (kN/mm)	229.7		
	Ductility	2.001		
SH100-3T	Maximum load (kN)	378.0	98.0	35.0
	Displacement (mm)	1.372	0.099	
	Stiffness (kN/mm)	261.1	31.4	13.67
	Ductility	1.841	-0.16	-8.00
SH100-1T 1L 1T	Maximum load (kN)	373.0	93	33.00
	Displacement (mm)	1.185	-0.088	
	Stiffness (kN/mm)	407.9	178.2	77.58
	Ductility	3.749	1.748	87.36
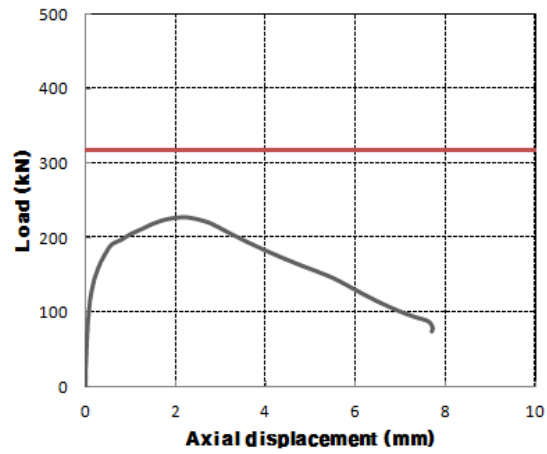
(a) SH60-0T
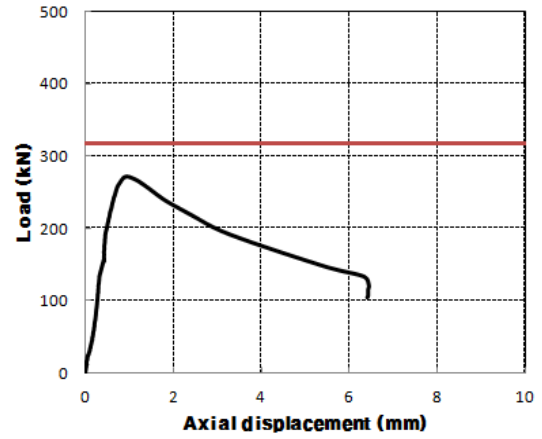
(b) SH60-1T
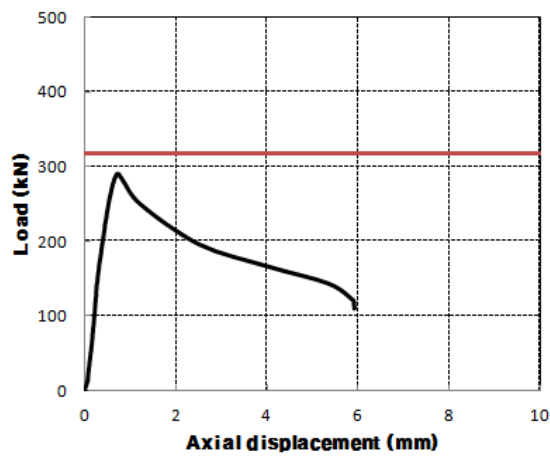
(c) SH60-3T
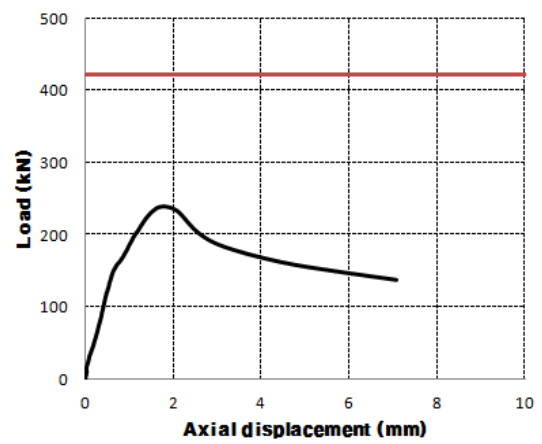
(d) SH80-0T
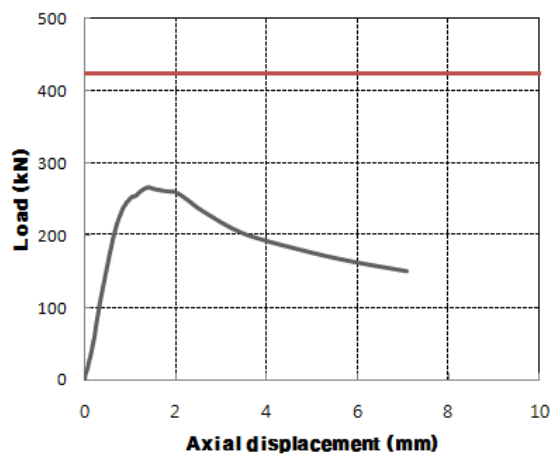
(e) SH80-1T
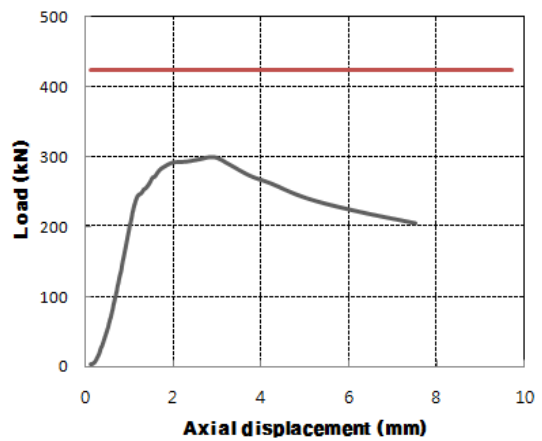
(f) SH80-3T

Fig. 4 Load-axial displacement curve

(g) SH100-0T
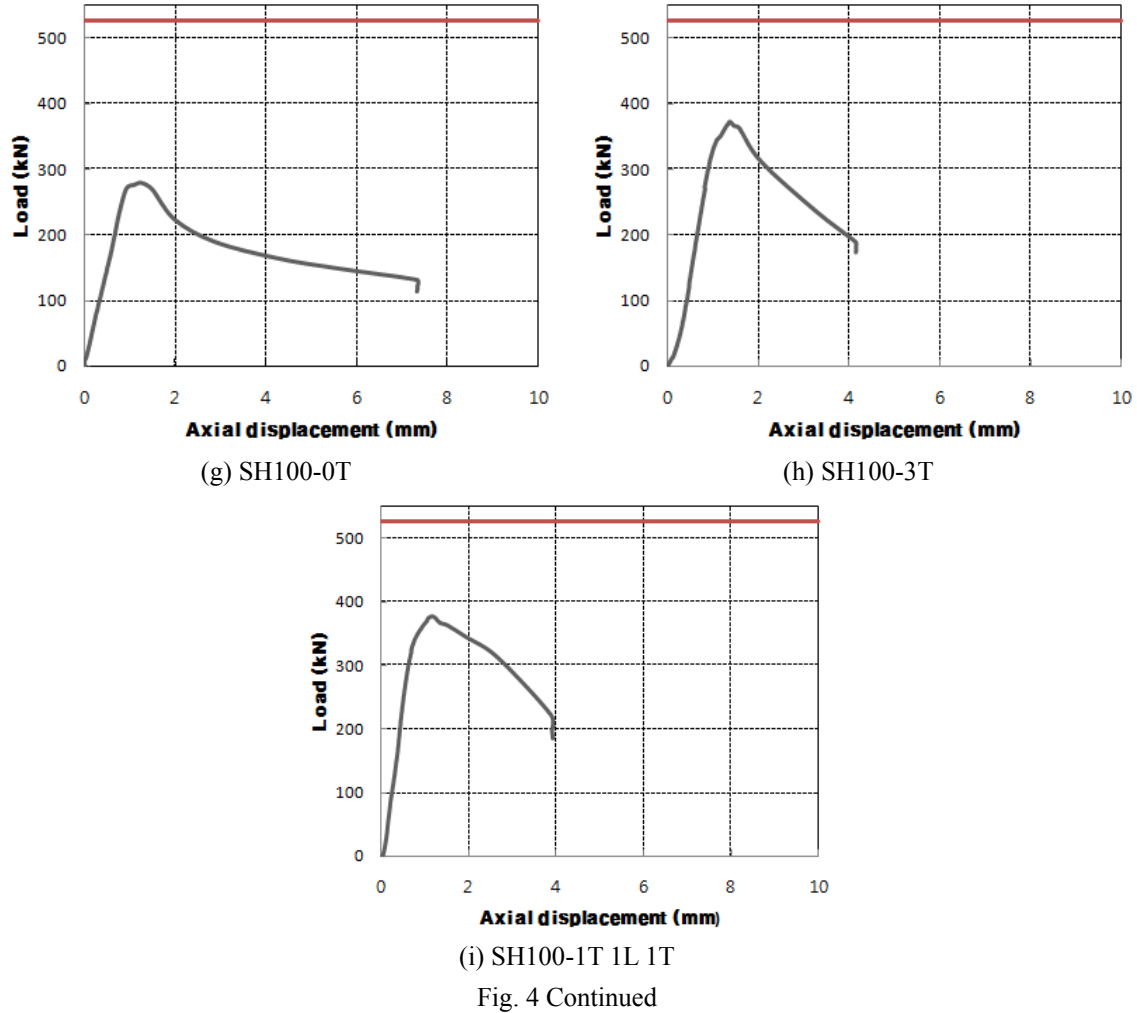

(h) SH100-3T

(i) SH100-1T 1L 1T

Fig. 4 Continued

Fig. 5 shows the measurement values of each strain gauge. The resulting values for the zone that caused large deformations on the surface of steel tube among the areas that have upper and lower gauges installed as shown in Fig. 2 were summarized, and load-strain curve for the axial strain and lateral strain were summarized. In examining the axial direction strain in Fig. 5, the axial strain of control specimen with $b/t = 60$ shows a gradual decrease in the internal strength after the point of maximum internal strength and thereby showing ductile behavior as compared to other specimens. However, specimens with large width-thickness ratio value ($b/t = 80$, $b/t = 100$) that are weak against local buckling show their inability to create large deformation after the point of maximum load and it is possible to observe the occurrence of elastic buckling where the load suddenly decreases. Nevertheless, in the specimens that are retrofitted with CFRP, as the number of CFRP ply increases in the specimens with $b/t = 80$, $b/t = 100$, the resulting values of lateral strain clearly increase and thereby making it possible to observe large deformations. Through these the fact that the CFRP retrofitting can delay local buckling and the load increase was verified.

When comparing the lateral strains of SH100 1T1L1T specimens and SH100-3T specimens, it was observed that relatively large deformations occurred for SH100 1T1L1T specimens, and through these it was verified that CFRP layers with fibers oriented in the transverse direction are more efficient in delaying local buckling than layers with fibers oriented in the longitudinal direction. The failure modes of specimens show at the same time the occurrence of inward local buckling and outward local buckling and the shape of failure, in the area where inward local buckling occurred the measured value of lateral strain gauge showed (–) strain values and the area where outward local buckling occurred (+) strain values, thereby making it possible to verify that the local buckling directions of specimens were occurring in different directions.
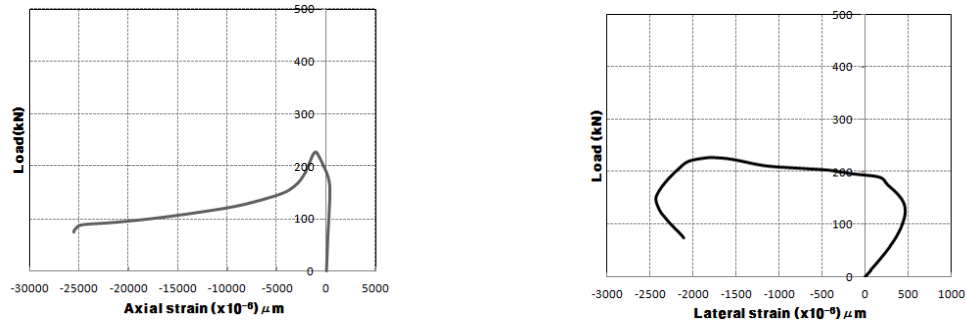
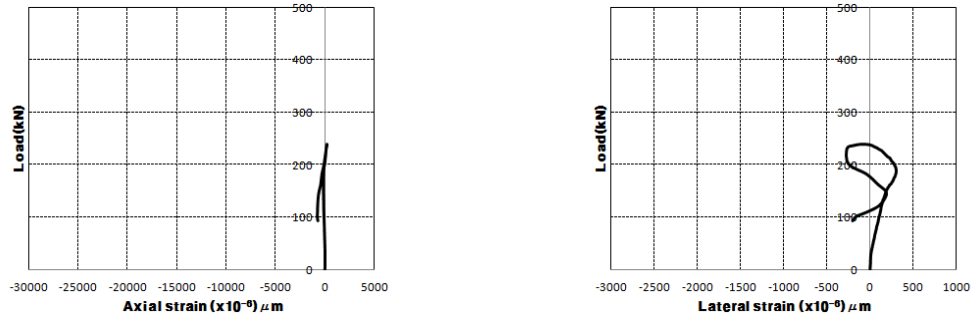(a) SH60-0T (gauges 7,8 inward local buckling)
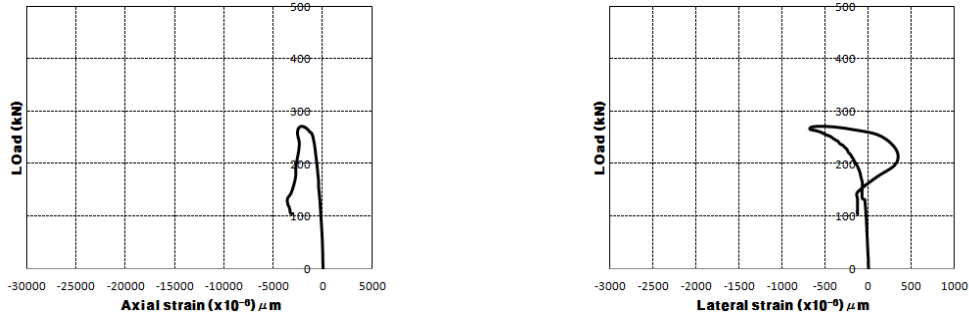
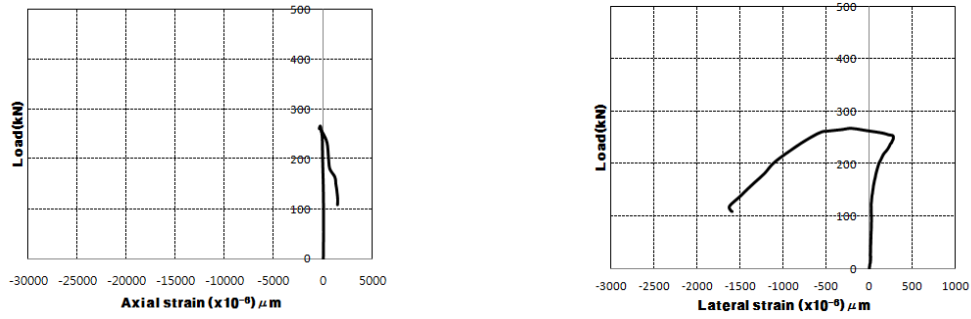(b) SH60-1T (gauges 5,6 inward local buckling)
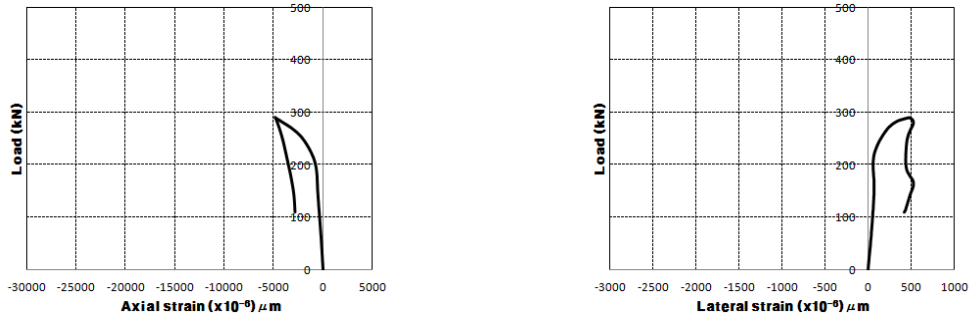
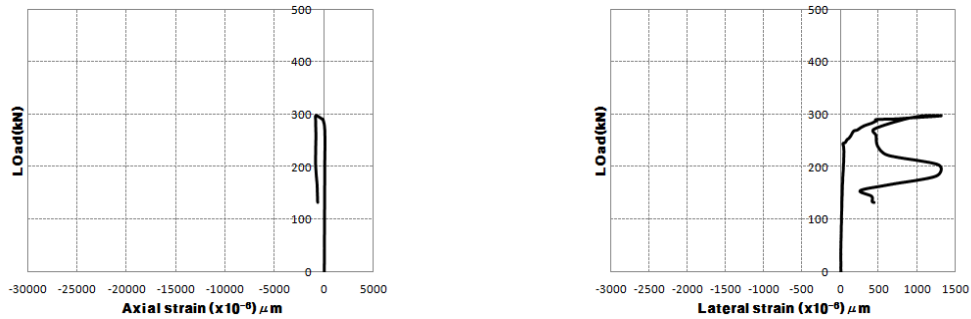(c) SH60-3T (gauges 5,6 outward local buckling)
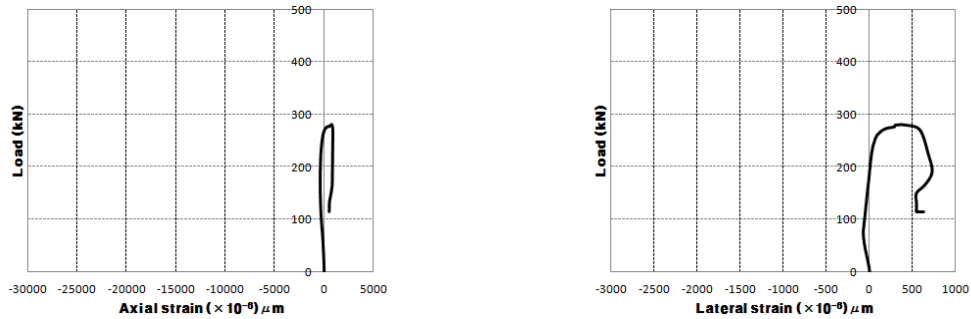
Fig. 5 Load-strain curve

(d) SH80-0T (gauges 5,6 inward local buckling)

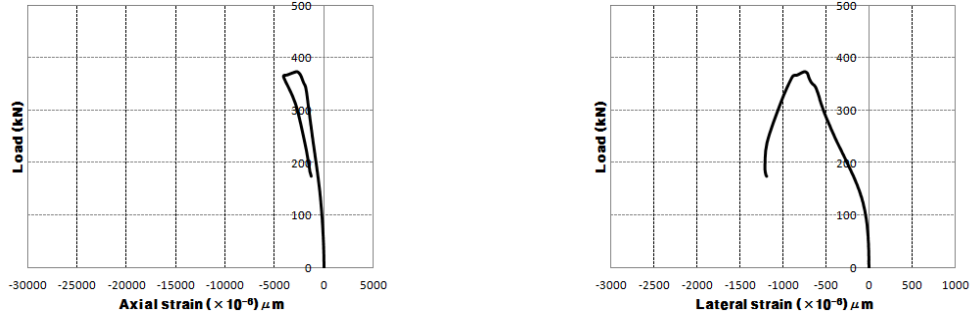(e) SH80-1T (gauges 5,6 inward local buckling)

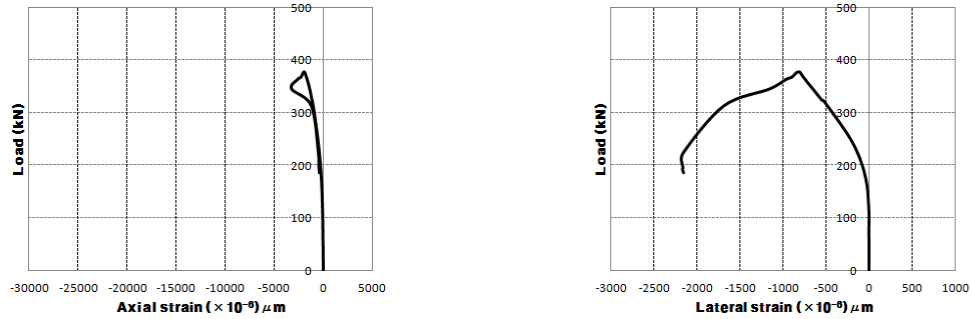(f) SH80-3T (gauges 5,6 outward local buckling)

(g) SH100-0T (gauges 7,8 outward local buckling)

Fig. 5 Continued

(h) SH100-3T (gauges 5,6 inward local buckling)

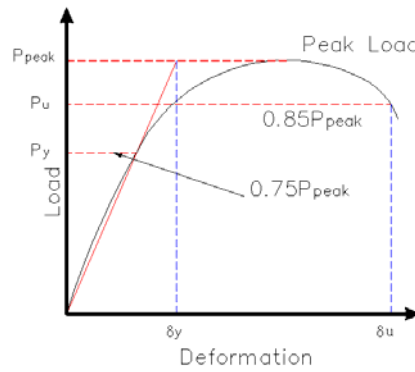(i) SH100-1T 1L 1T (gauges 5,6 inward local buckling)

Fig. 5 Continued

Fig. 6 Definition of ductility (Hu 2010)

3.3 Stiffness and ultimate load capacity

Stiffness is defined as shown in Eq. (1) and the concept of stiffness is shown in Fig. 6 (Tao *et al.* 2007).

$$K_y = \frac{P_y}{\delta_y} \qquad (1)$$

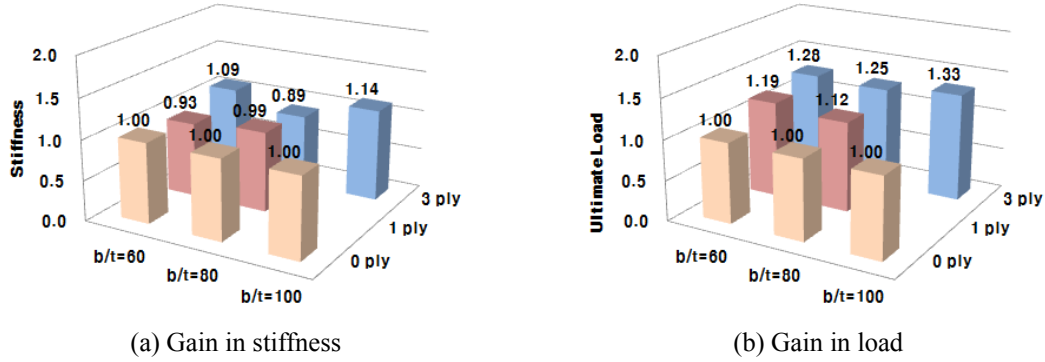(a) Gain in stiffness   (b) Gain in load

Fig. 7 Effect of number of CFRP layer on stiffness and ultimate load

Stiffness was seen to be increasing or decreasing by within 10% as compared to the control specimen, as shown in Fig. 7(a), and the number of CFRP ply was seen as being unable to affect the stiffness. For the ultimate load capacity, as shown in Fig. 7(b), in accordance with increasing number of CFRP ply, based on the width-thickness ratios, each increased by 27%, 25% and 30%, and it was verified that CFRP retrofitting in the transverse direction contributed to increase in the load capacity. This is indicating a tendency that specimens with large plate width-thickness ratios are relatively weak against local buckling and thereby the load decreases before reaching the yield load; however, CFRP retrofitting could delay local buckling, which is thought to be attributable to an increase in the load capacity through an increase in the elastic buckling stress.

3.4 Ductility

Ductility is defined using the yield point (δ_y) and failure point (δ_u) obtained in Figure 6 and this is shown in Eq. (2). The failure point (δ_u) is defined as the point at which the internal strength is decreased by 85% after the point of maximum internal strength (Schneider 1998). The yield point and failure point are calculated through the load-axial displacement curve in Fig. 6 and the calculated DI (ductility index) values are summarized in Table 2.

$$DI = \frac{\delta_u}{\delta_y} \tag{2}$$

The results of effects of number of DI (ductility index) depending on the number of CFRP ply are summarized in Fig. 8. DI (ductility index) was seen to be generally decreasing as the number of CFRP ply increased. Except in the case of SH80-3T specimens, it was seen to be increasing by about 5% as compared to the control specimen. As can be seen in Fig. 8, specimens with a small width-thickness ratio ($b/t = 60$), the DI decrease rate was shown to be larger. This can be thought as, in the case of specimens with a small width-thickness ratio ($b/t = 60$), because they have a relatively large amount of steel, the ductile behavior is maintained after the point of maximum load. However, in the case of the other 2 specimen groups ($b/t = 80$, $b/t = 100$), because they have a relatively low amount of steel, they cannot produce ductile behavior and, due to the brittle properties of CFRP, after all, the DI decreased.
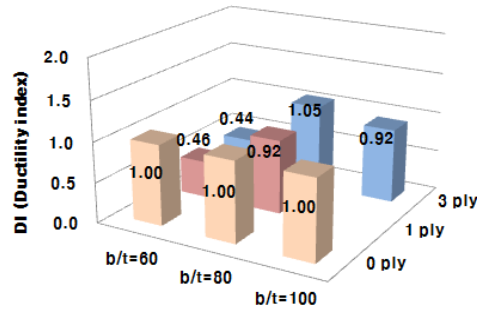
Fig. 8 Effect of number of CFRP layer on ductility

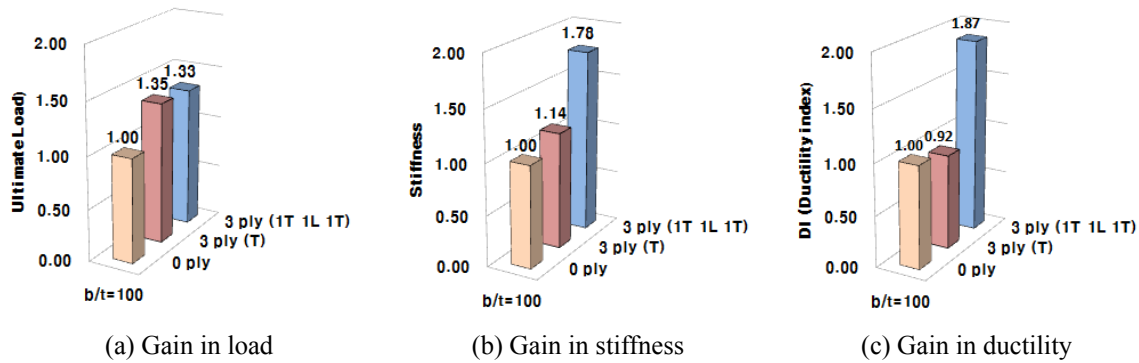| (a) Gain in load | (b) Gain in stiffness | (c) Gain in ductility |

Fig. 9 Effect of fiber orientation on ultimate load, stiffness and ductility

3.5 Effect of fiber orientation on ultimate load, stiffness and ductility

Of the specimens with a width-thickness ratio of 100, in order to ascertain the effects of fiber orientation, 1 specimen was retrofitted using CFRP in alternating fashion: the transverse direction, longitudinal direction and transverse direction, and the resulting load effects are summarized in Fig. 9. As can be seen in Fig. 9, in the case of the specimens (SH100-3T) retrofitted with 3-layers in the transverse direction and the specimens (SH100-1T 1L 1T) retrofitted in alternating fashion, when compared to the control specimen their internal strength increase rates were seen to be similar, however, their stiffness and ductility increase rates increased by 78% and 87%, respectively, when compared to the control specimen, thereby showing that the stiffness and ductility capacity could be improved when compared to the specimens retrofitted in the transverse direction only.

3.6 Discussion of failure mode

Fig. 10 shows the shapes of final destruction of each of the specimens. As can be seen in the figure, it can be verified that local buckling occurs in the upper region or lower region of specimens, and also can be verified is that, of the total 4 sides, 2 sides undergo inward local buckling and the other 2 sides undergo outward local buckling.

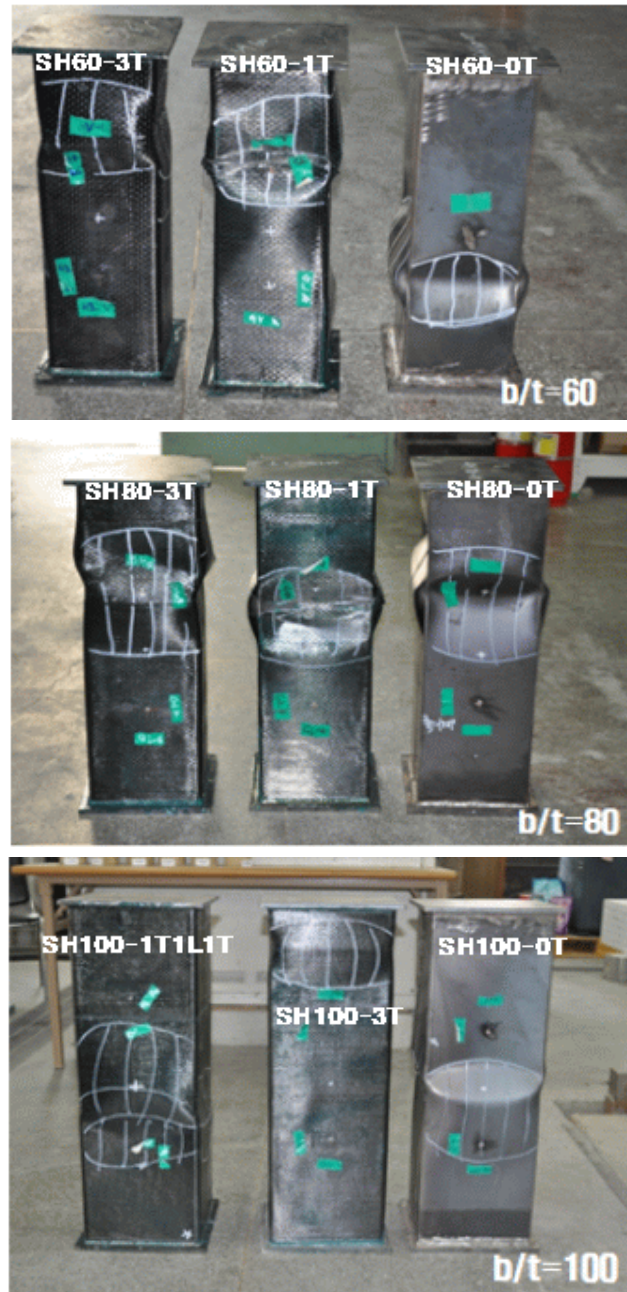Fig. 10 Final failure shape

Fig. 11 shows a schematic of typical failure mode for short HSS columns. From the test, it was observed that two sides would typically buckle outward and the other two sides would buckle inward. In this study, for thin-walled sections, this type of deformation occurs before the cross-sectional yield capacity is reached. In Fig. 11, it can be observed that FRP sheets could
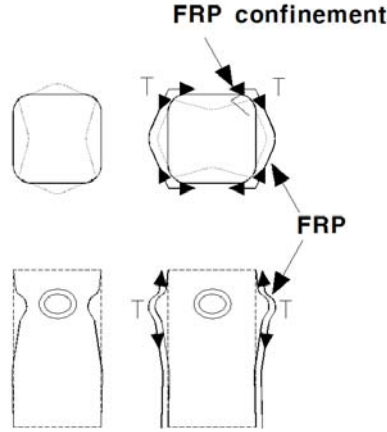
Fig. 11 Schematic of typical failure mode for a short SHS column

confine outward buckling and that transverse FRP layers are effective in confining outward local buckling of the two opposite steel sides. This confinement controls local buckling of HSS columns, and it can improve the axial capacity of HSS columns. However, in Fig. 11, it could not be observed that FRP sheets contribute much to the sides that buckle inward. On the sides, delamination of the FRP sheet tends to occur, and it is not expected that FRP sheet can confine steel plate and control inward local buckling.

4. Prediction of axial load capacity

4.1 Elastic buckling results

SHS may be considered as stiffened plates that are simply supported along the longitudinal edges. The slenderness ratio (λ) is defined in Eq. (3) and the elastic buckling stress (f_{cr}) is defined in Eq. (4) (Akesson 2007).

$$\lambda = \sqrt{\frac{f_y}{f_{cr}}} \tag{3}$$

$$f_{cr} = \frac{k\pi^2 E}{12(1-v^2)}(\frac{t}{b})^2 \tag{4}$$

Where, f_y is the yield stress of steel plate, E is Young's modulus, t is the plate thickness, b is the inner plate width, v is the Poisson's ratio, and k is the elastic buckling coefficient (for stiffened elements, k is 4.0).

In this study, elastic buckling stress (f_{cr}) was determined from the test results of load-axial displacement curve. From load-axial displacement curve, elastic buckling stress is determined as the maximum load at which the curve changes slope, and this is because the load is reduced when a section buckles. The experimental results of elastic buckling stress and plate slenderness ratio are

Table 3 Experimental and theoretical results for SHS and CFRP-SHS columns

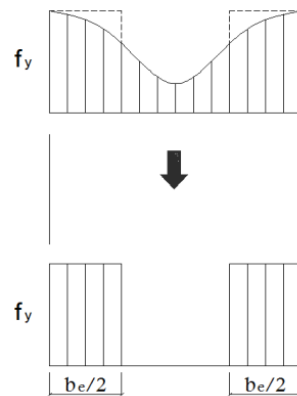| Specimen label	b/t (Actual value)	Steel slenderness, Eq. (3)	EXP steel slenderness	EXP slenderness	Exp. buckling stress (MPa)	Reduction factor (ρ)	Exp. capacity (kN)	Theory capacity (kN)	$\frac{P_{EXP}}{P_{uc}}$
SH60-0T				1.22	192.22	0.67	227.0	227.8	0.99
SH60-1T	62.7	1.25	1.22	1.12	229.47	0.80	271.0	272.1	1.00
SH60-3T				1.08	245.56	0.84	290.0	285.7	1.02
SH80-0T				1.37	152.41	0.53	239.0	275.5	0.87
SH80-1T	83.6	1.66	1.37	1.30	170.26	0.68	267.0	307.1	0.87
SH80-3T				1.23	190.03	0.69	298.0	311.6	0.96
SH100-0T	104.5	2.08	1.42	1.42	143.20	0.49	280.0	332.2	0.84
SH100-3T	104.5	2.08	1.42	1.22	193.31	0.65	378.0	366.0	1.03
								Mean:	0.95
								Cov:	0.076

Fig. 12 Plate elements under axial compression (Akesson 2007)
(Actual stress distribution and equivalent distribution)

presented in Table 3. From the test results, it is evident that additional layers of CFRP provide additional increase in elastic buckling stress and decrease the slenderness ratio. The increase in buckling stress provided by the addition of CFRP may be considered the result of restriction of buckling deformation provided by CFRP.

4.2 Capacity prediction using proposed strength curves

In this chapter, the strength curves of CFRP strengthened steel plate are proposed to predict the ultimate load capacity of CFRP strengthened SHS columns.

In rectangular steel tubes comprised of thin-wall elements, by using the actual state of stress distribution through utilizing the concept of effective width (b_e) and a reduction factor (ρ), they are substituted with equivalent state of stress distribution to calculate compressive strength, and the concept of this is shown in Fig. 12.

(a) Plain steel plates
(Winter strength curve)

(b) FRP strengthened steel plates
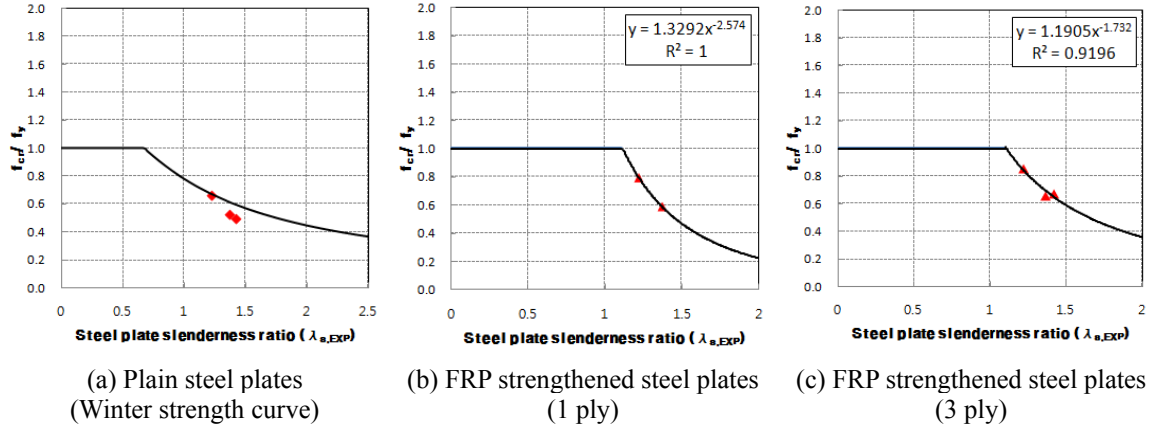(1 ply)

(c) FRP strengthened steel plates
(3 ply)

Fig. 13 Displacements of the girders and the columns according to time (1st test)

In order to obtain the ultimate load-carrying capacity, we used expressions for effectiveness width. The ultimate load-carrying capacity can be expressed as in Eq. (5).

$$P_{uc} = f_y b_e t \tag{5}$$

The effective width is calculated as the original steel width times the reduction factor, as shown in Eq. (6).

$$b_e = \rho b \tag{6}$$

For plain steel plates, the reduction factor (ρ) is predicted by the Winter strength Eq. (7), which is to be expected since this is the approach taken by the American specifications for cold-formed steel structures (AISI Standard 2001) and is known to be reliable (Akesson 2007). Also, in this study, the resulting reduction factors for FRP-steel plates are given, respectively, by Eqs. (8) and (9) and are plotted in Fig. 13. The values of steel plate slenderness (λ) can be derived from test results for plain steel plates and is listed in Table 4. In Fig. 13, the reduction factor (ρ) is plotted against the experimental non-dimensional strength for steel plates reinforced with CFRP and also is compared with the test results. Finally, the theory-based axial capacity (P_{uc}) is presented in Table 3 and is also compared with the test results (P_{EXP}).

For plain steel plates

$$\rho = \frac{f_y}{f_{cr}} = \frac{1 - \dfrac{0.22}{\lambda}}{\lambda} \tag{7}$$

For steel plates reinforced with 1-ply CFPR

$$\rho = \frac{f_y}{f_{cr}} = \frac{1.329}{\lambda^{2.574}} \tag{8}$$

For steel plates reinforced with 3-ply CFPR

$$\rho = \frac{f_y}{f_{cr}} = \frac{1.191}{\lambda^{1.732}}$$

(9)

5. Conclusions

In this study, 9 specimens of SHS columns comprised of thin-walled elements were retrofitted with CFRP in the transverse direction and in alternating fashion in the transverse direction and longitudinal direction were fabricated and central compression tests were conducted. The test variables were the width-thickness ratio, the number of CFRP ply and fiber orientation. From the axial load tests, the structural behavior was observed, and the effect of CFRP wrap, initial stiffness, ductility, etc. were compared. The conclusions derived in this study are as follows.

1. Regarding the SHS short columns, through reinforcement in the transverse direction using CFRP sheet, outward local buckling can be confined and thereby delaying the local buckling, and as a result of this, the axial load capacity is increased. However, regarding the side that sees inward local buckling, CFRP undergoes delamination and CFRP sheet delamination is unable to contribute in controlling local buckling against inward local buckling.

2. In examining the load-axial displacement curves, since all the specimens have large width-thickness ratios, local buckling occurs before reaching the yield load, and because of this, elastic buckling behavior in which the load decreases is displayed. Although all the specimens show a trend of gradual decrease in the internal strength after the point of maximum load, the SH100-3T and SH100-1T1L1T specimens show a tendency of suddenly decreasing load after the point of maximum load.

3. In the load-strain response, generally, strain in the axial direction does not undergo large deformations after the maximum load point and showed decreasing load, and all the specimens showed elastic buckling behavior in which the yield load is not reached. In examining strain in the transverse direction, as the number of CFRP ply increased, the values of strain in the transverse direction clearly increased, and because of this, the occurrences of large deformations were observable. Through this, the fact that retrofitting using CFRP can delay local buckling was ascertained.

4. A maximum increase of 33% was achieved in axial-load capacity when 3-layers of CFRP were used to wrap transversely the HSS columns of $b/t = 100$. However, the compressive internal strength increase rate for specimens that were reinforced with 3-layers of CFRP in alternating fashion was similar to that of specimens that were retrofitted with 3-layers in the transverse direction only, thereby indicating that the fiber orientation does not affect increased in the axial load capacity.

5. In the specimens that were reinforced in the transverse direction only, the stiffness was almost constant with about a 10% deviation even as the number of CFRP ply increased, which verified that retrofitting using CFRP does not affect the stiffness. However, as the number of CFRP ply increased, the ductility index (DI) was seen to decrease and this type of phenomenon was clearly shown in specimens with a small width-thickness ratio ($b/t = 60$). Nevertheless, in the case of specimens with retrofitting in alternating fashion, the stiffness and DI increase rates were shown to be 78% and 85%, respectively, which enabled verification that the fiber orientation contributes to the stiffness and DI increases.

6. Lastly, based on the test results, by applying the reduction factors on thin-walled rectangular

tubes that are retrofitted with CFRP, elastic buckling stress prediction equation was proposed, and based on this, the ultimate load capacity was predicted. Since the prediction equation was very close to the actual test values, it is thought that the equation is reliable.

References

AISC (2005), Steel Construction Manual, Vol. 2, (13th Ed.) American Institute of Steel Construction.

AISI Standard (2001), Supplement to the North American Specification for the Design of Cold-Formed Steel Structural Members, American Iron and Steel Institute.

Akesson, B. (2007), *Plate Buckling in Bridges and Other Structures*, Taylor & Francis, UK, 14-17.

El-Tawil, S., Ekiz, E., Goel, S. and Chao, S.H. (2011), "Retraining local and global buckling behavior of steel plastic hinges using CFRP", *J. Construct. Steel Res.*, **67**(3), 261-269.

Fam, A., Macfougall, C. and Shaat, A. (2009), "Upgrading steel-concrete composite girders and repair of damaged steel Beams using bonded CFRP laminates", *Thin-Walled. Struct.*, **47**(10), 1122-1135.

Harries, K.A., Peck, A.J. and Abraham, E.J. (2009), "Enhancing stability of structural steel sections using FRP", *Thin-Walled. Struct.*, **47**(10), 1092-1101.

Hu, Y.M. (2010), "Behavior and modeling of FRP confined hollow and concrete-filled steel tubular columns", Ph.D. Thesis, Hong Kong Polytechnic University, 35.

Miller, T.C., Chajes, M.J., Mertz, D.R. and Hastings, J.N. (2001), "Strengthening of a steel bridge girder using CFRP plates", *ASCE, J. Bridge. Eng.*, **6**(6), 514-522.

Narmashri, K., Jumaat, M.Z. and Sulong, N.H.R. (2010), "Shear strengthening of steel I-beams by using CFRP strips", *Scientif. Res. Essays.*, **5**(16), 2155-2168.

Sallam, H.E.M., Badawy, A.A.M., Saba, A.M. and Mikhail, F.A. (2010), "Flexural behavior of strengthened steel-concrete composite beams by various plating methods", *J. Const. Steel Res.*, **66**(8-9), 1081-1087.

Schneider, S.P. (1998), "Axially loaded concrete-filled steel tubes", *ASCE, J. Struct. Eng.*, **124**(10), 1125-1138.

Shaat, A. and Fam, A.Z. (2006), "Axial loading tests on short and long hollow structural steel columns retrofitted using carbon fibre reinforced polymers", *Can. J. Civil Eng.*, **33**(4), 458-470.

Shaat, A. and Fam, A.Z. (2009), "Slender steel columns strengthened using high-modulus CFRP plates for buckling control", *ASCE, J. Compos. Const.*, **13**(1), 2-12.

Tao, Z., Han, L.H. and Zhung, J.P. (2007), "Axial Load Behavior of CFRP Strengthened Concrete-Filled Steel Tubular Stub Columns", *Adv. Struct. Eng.*, **10**(1), 37-46.

Teng, J.G. and Hu, Y.M. (2007), "Behavior of FRP-Jacked Circular Steel Tubes and Cylindrical Shells under Axial Compression", *Const. Build. Mater.*, **21**(4), 827-838.

CC